Available online at www.sciencedirect.com

ScienceDirect

Procedia Computer Science 100 (2016) 1141 – 1146

Procedia Computer Science

Conference on ENTERprise Information Systems / International Conference on Project MANagement / Conference on Health and Social Care Information Systems and Technologies, CENTERIS / ProjMAN / HCist 2016, October 5-7, 2016

Multi-sensor InSAR analysis of surface displacement over coastal urban city of Trondheim

Roghayeh Shamshiri[a,*], Hossein Nahavandchi[a], Mahdi Motagh[b], Mahmud Haghshenas Haghighi[b]

[a]*Department of Civil and Transport Engineering, NTNU, Norwegian University of Science and Technology, 7491 Trondheim, Norway*
[b]*GFZ German Research Centre for Geosciences, 14473 Potsdam, Germany*

Abstract

In this study, we present maps of ground surface displacement of the coastal urban city of Trondheim in central Norway using observations from interferometry synthetic aperture radar (InSAR). We used 98 SAR images including 31 TerraSAR-X, 49 Radarsat-2, and 18 Sentinel-1 to assess mean deformation velocity maps and displacement time-series in the city between 2012 and 2016. We processed the data using InSAR time-series technique of Small BAseline Subset (SBAS) approach. The results show that the displacement with the maximum value of approximately -15 mm/yr has been happening on the coastal area since 2012. However, in the rest of the city displacement patterns vary in different time-periods. The displacement velocity in the city ranged from -10 to +2 mm/yr in 2012-2014, -4 to +2 mm/yr in 2012-2015, and -7 to +7 mm/yr in 2015–2016 in the line of sight (LOS) direction.

Peer-review under responsibility of the organizing committee of CENTERIS 2016

Keywords: Multi-sensor; InSAR; Trondheim; displacement.

* Corresponding author. Tel.: +47-98309174
E-mail address: roghayeh.shamshiri@ntnu.no

Peer-review under responsibility of the organizing committee of CENTERIS 2016
doi:10.1016/j.procs.2016.09.267

1. Introduction

Trondheim city is located in central Norway. It is a coastal city, lying on the south shore of the Trondheim Fjord and the river Nidelva runs through the city (see Fig. 1). Flood, erosion and landslide naturally occur in and along Norwegian rivers and may cause considerable damage to houses, roads and other infrastructure situated along the river. For instance, in January 2012, a massive landslide took place just south of Trondheim leading to evacuation order of people from a rural area.

In regions like Trondheim, risk managers and local administrations need ground deformation maps to plan effective prevention measures and implement warning systems. Even if ground deformation cannot be prevented or stopped, it must be accounted for in new construction planning.

Identification and monitoring of ground deformation can be accomplished using a number of surveying techniques. These techniques have been evolved using Global Navigation Satellite Systems (GNSS)[1-3], but for large areas, the use of GNSS and leveling are time consuming, expensive and laborious. In contrast to the surveying techniques that rely on point measurements at the Earth surface, Interferometric Synthetic Aperture Radar (InSAR) overcomes many practical limitations and readily provides high-resolution measurements of sub-cm accuracy over relatively large areas[4-6]. Advanced time-series techniques of Persistent Scatterer (PS) and small baseline methods[7-9] enable the retrieval of deformation time-series and velocity maps from SAR data[10-14].

In this study, we use 98 SAR images from TerraSAR-X, Radarsat-2, and Sentinel-1 to assess deformation during 2012–2016. The data is processed using InSAR time-series technique of Small BAseline Subset (SBAS) approach, implemented in StaMPS software (http://radar.tudelft.nl/~ahooper/stamps).

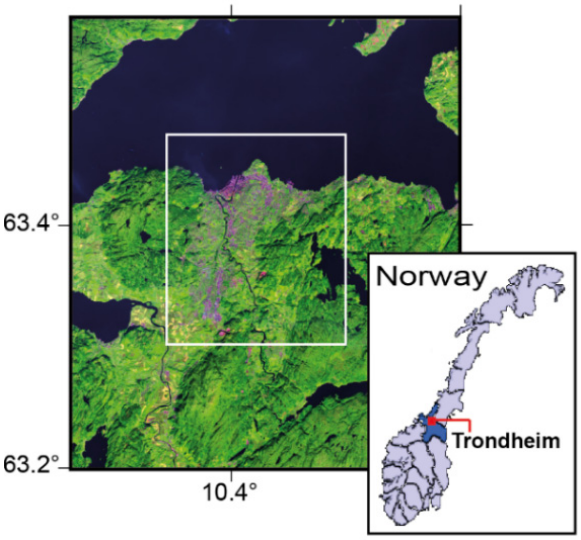

Fig. 1. Landsat-8 image of the study area. Inset at the bottom right indicates the location of Trondheim city in Norway. The white rectangle shows the area of interest.

Nomenclature

GNSS	Global Navigation Satellite Systems
SAR	Synthetic Aperture Radar
InSAR	Interferometric Synthetic Aperture Radar
PSI	Persistent Scatterers Interferometry
SBAS	Small BAseline Subset
StaMPS	Stanford Method for Persistent Scatterers

LOS	Line of sight of satellite
SDFP	Slowly Decorrelating Filtered Phase

2. Data and methodology

The SAR dataset used in this study consists of 31 TerraSAR-X data in a descending track covering January 2012–March 2014, 49 Radarsat-2 data in an ascending track covering March 2012–October 2015, and 18 Sentinel-1 data in an ascending track covering Jun 2015–May 2016. Fig. 1 illustrates the outline of the processed area with different satellites. We performed time-series analysis of SBAS approach implemented in StaMPS software. The processing method includes three main steps. Firstly, we created the networks with 82, 280, and 67 differential interferograms using data from TerraSAR-X, Radarsat-2, and Sentinel-1, respectively, with minimal spatial, temporal and Doppler baselines. The interferograms of the TerraSAR-X and Radarsat-2 data have been produced using the repeat-pass technique implemented in DORIS[15]. For the Sentinel-1 data we used Gamma[16] software to produce the interferograms. The digital terrain model is provided by the Norwegian Mapping Authority with a resolution of 10 m for topography phase correction and geocoding.

Having made the differential small baseline interferograms, the next step is selecting the Slowly Decorrelating Filtered Phase (SDFP) pixels. As there is a correlation between amplitude stability and phase stability, for the sake of computational efficiency, an initial selection of SDFP pixels is implemented in StaMPS using the amplitude difference dispersion index threshold. The index is the standard deviation of the amplitude difference between the master and slave divided by the mean amplitude, which was set to 0.6 in this study. Using an iterative statistical process the final set of SDFP pixels were selected.

In the third step, a three-dimensional phase unwrapping was applied on the selected SDFP pixels[17]. Finally, a least-squares inversion was carried out to derive the displacement time-series. Further details regarding StaMPS can be found in the relevant literature[9, 18].

One of the main challenges in InSAR processing is related to atmospheric delays. A temporal change in the amount of atmospheric water vapor between the acquisition times of SAR images affects the refractive index of the atmosphere and induces a propagation delay. Part of the atmospheric artifacts have been accounted for in the computations in StaMPS. The computation technique has proven to be effective in the mitigation of atmospheric artifacts when a long time-series of interferograms are used as it is the case in this study. However, complexity of our study area requires further investigation of atmospheric effects[19-22].

3. Results and discussion

Fig. 2 shows the displacement velocity maps along the line of sight (LOS) direction using TerraSAR-X (Fig. 2a), Radarsar-2 (Fig. 2b), and Sentinel-1 (Fig. 2c). As it can be seen, the displacement with the maximum value of approximately -15 mm/yr is happening on the coastal area during 2012-2016. However, in the rest of the city displacement patterns vary in different time-periods.

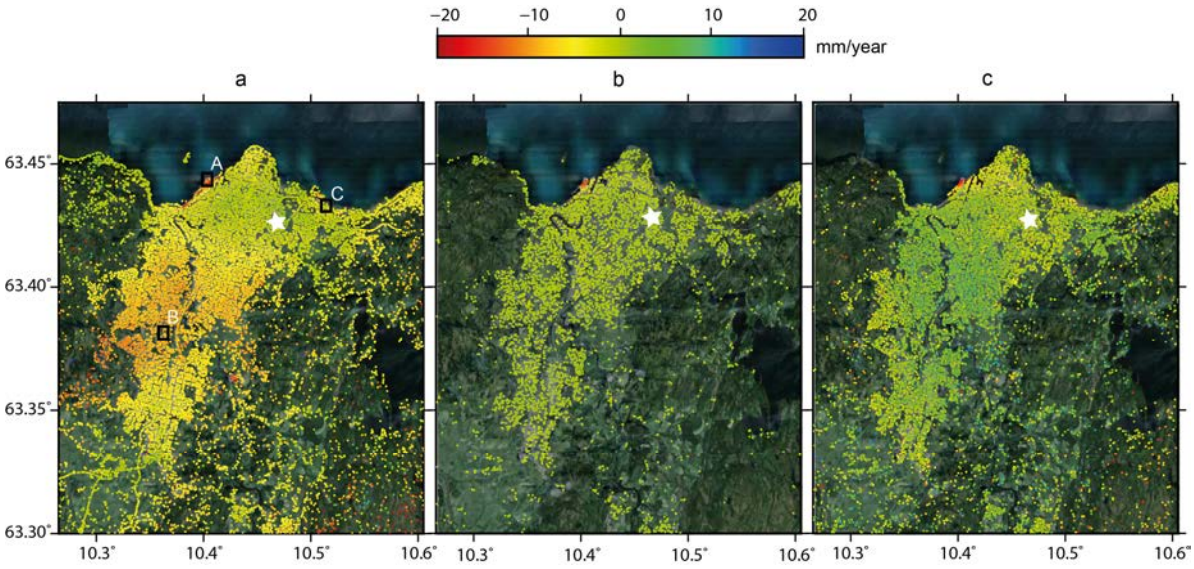

Fig. 2. Average displacement velocity maps along the LOS direction in the year (a) 2012-2014, (b) 2012-2015, (c) 2015-2016 derived from TerraSAR-X, Radarsat-2, and Sentinel-1 data, overlaid on Google Earth image. The velocities are relative to the white star reference point, which is assumed to be stable.

Part of these differences in LOS velocity arises from different imaging geometries that cause different sensitivity to the vertical and horizontal displacements. The unit vector of the LOS direction in the coordinate system (east, north, up) is approximately (0.43, -0.1, 0.89) for TerraSAR-X, (-0.33, 0.1, 0.94) for Radarsat-2 and (-0.48, −0.1, 0.87) for Sentinel-1 data in this study. This shows that the sensors are most sensitive to the vertical displacement, but east-west displacement will cause LOS change with opposite sign on descending (Radarsat-2 and Sentinel-1) and ascending (TerraSAR-X) results. Some other part of the differences are related to the atmospheric artifacts.

However, the most part of the difference in LOS velocity maps is because of the different displacement patterns in different years. Therefore, the LOS velocity maps alone are not useful in interpreting the results. Time-series of displacement should be considered as well.

To compare three sets of displacement time-series, we converted LOS of each observation to the vertical direction by ignoring the horizontal components. The three time-series were computed using one master scene for each dataset. The temporal reference is the master date. To combine the vertical displacement of the three datasets, we have to account for relative ground displacement between the master dates in the three time series. For this, we fitted a linear trend to each of the time-series and calculated the shifts between datasets. The results of which for three areas relevant to the points labelled A, B, and C in Fig. 2a have been illustrated in Fig. 3. As it can be seen, the three series follow each other closely. The time-series of the point A, located in coastline depicts that the area is subsiding steadily with the cumulative displacement of approximately 8 cm during 2012-2016 (Fig. 3a). This area is the river delta and has been filled by different kinds of building materials up to 5-10 m depth. Therefore, it is at the preliminary consolidation steps.

The time-series of the point B, which is a clayey area located beside the river, shows that the area subsided until the mid-2014 by approximately 3 cm, its rate is decreased until the mid-2015, and it is subsided again by 2 cm with some fluctuations until mid-2016 (Fig. 3b). The Fig. 3c shows the time-series of the point C, which is situated close to the coast. As it can be seen, the area has been affected by short-term fluctuations in sinus cycle. It rises in winter and goes down in summer.

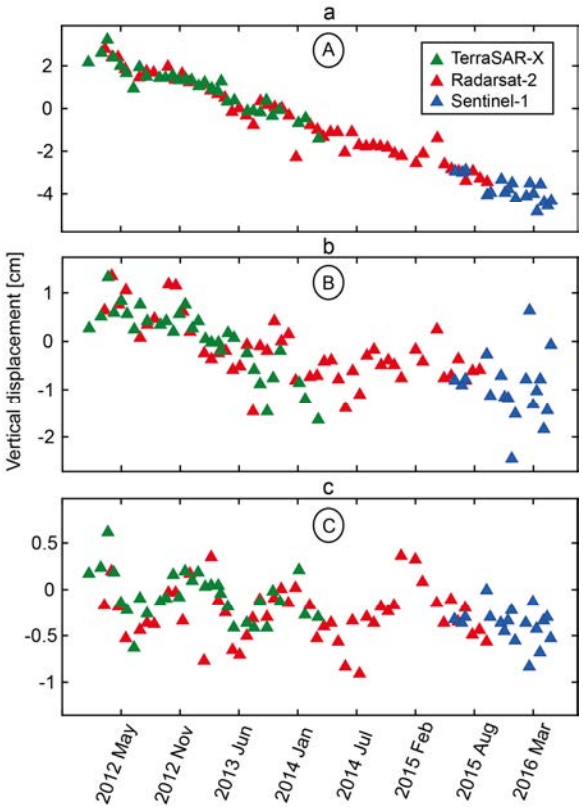

Fig. 3. Vertical displacement time-series derived from TerraSAR-X (the green triangles), Radarsat-2 (the red triangles), and Sentinel-1 (the blue triangles) data between 2012 to 2016, in points (a) A, (b) B, and (c) C (the location of the points has been shown in Fig. 2a).

4. Conclusion

InSAR analysis is an effective technique to map surface deformation with high spatial resolution. We used X-band and C-band InSAR time-series survey to monitor the displacement in Trondheim city, Norway. The result of InSAR analysis shows that the ground monitoring of an urban city can be performed with high precision. Moreover, detection of the parts where the collapse is expected to occur in the near future is also possible. The results here presented suggest that the InSAR technique can offer information useful to build up a monitoring and identification system.

The results showed the displacement with peak amplitude of approximately -15 mm/yr has been occurring on the coastal area since 2012. In the rest of the city displacement patterns vary in different time-periods. Vertical displacement time-series derived from TerraSAR-X, Radarsat-2, and Sentinel-1 data between 2012 to 2016 follow each other closely. The reason of displacements in urban areas, especially coastal cities like Trondheim is a challenging task. Several factors can be considered to explain displacements. Among them, hydrological factors, climate, and surface roughness. It should also be mentioned that the study area experiences post glacial rebound of around 4 mm/yr (however, the relative uploading rate is approximately 0.5 mm/yr). The study area experiences severe temperature changes. Temperature differences in the imaged area between two SAR acquisitions add a thermal component to interferograms, which needs to be analyzed with care for deformation analysis in urban areas (see e.g.[23, 24]).

Acknowledgements

We would like to thank the German Aerospace Agency (DLR) for acquiring and providing TerraSAR-X data under the research project motagh_GEO1916, the European Space Agency (ESA) for supplying the Sentinel-1 images, and the Norwegian Space Center (NSC)/Kongsberg Satellite Service (KSAT) for providing Radarsat-2 data under the Norwegian-Canadian Radarsat agreement (2016).

References

1. Lovse J, Teskey W, Lachapelle G, Cannon M. Dynamic deformation monitoring of tall structure using GPS technology. *Journal of surveying engineering* 1995; 121: 35-40.
2. Zhenghang L, Zhizhao L, Zemin W. Study on monitoring dam deformation with GPS positioning [J]. *Journal of Wuhan University of Hydraulic and Electric Engineering* 1996; 6.
3. Ustun A, Tusat E, Yalvac S. Preliminary results of land subsidence monitoring project in Konya Closed Basin between 2006–2009 by means of GNSS observations. *Natural Hazards and Earth System Sciences* 2010; 10: 1151-1157.
4. Motagh M, Schurr B, Anderssohn J, Cailleau B, Walter TR, Wang R, Villotte J-P. Subduction earthquake deformation associated with 14 November 2007, Mw 7.8 Tocopilla earthquake in Chile: Results from InSAR and aftershocks. *Tectonophysics* 2010; 490: 60-68.
5. Wright TJ, Parsons BE, Lu Z. Toward mapping surface deformation in three dimensions using InSAR. *Geophysical Research Letters* 2004; 31.
6. Bechor NB, Zebker HA. Measuring two-dimensional movements using a single InSAR pair. *Geophysical research letters* 2006; 33.
7. Ferretti A, Prati C, Rocca F. Permanent scatterers in SAR interferometry. *Geoscience and Remote Sensing, IEEE Transactions on* 2001; 39: 8-20.
8. Berardino P, Fornaro G, Lanari R, Sansosti E. A new algorithm for surface deformation monitoring based on small baseline differential SAR interferograms. *Geoscience and Remote Sensing, IEEE Transactions on* 2002; 40: 2375-2383.
9. Hooper A. A multi-temporal InSAR method incorporating both persistent scatterer and small baseline approaches. *Geophysical Research Letters* 2008; 35.
10. Ferretti A, Prati C, Rocca F. Nonlinear subsidence rate estimation using permanent scatterers in differential SAR interferometry. *Geoscience and Remote Sensing, IEEE transactions on* 2000; 38: 2202-2212.
11. Colesanti C, Ferretti A, Prati C, Rocca F. Monitoring landslides and tectonic motions with the Permanent Scatterers Technique. *Engineering Geology* 2003; 68: 3-14.
12. Motagh M, Hoffmann J, Kampes B, Baes M, Zschau J. Strain accumulation across the Gazikoy–Saros segment of the North Anatolian Fault inferred from Persistent Scatterer Interferometry and GPS measurements. *Earth and Planetary Science Letters* 2007; 255: 432-444.
13. Motagh M, Wetzel H-U, Roessner S, Kaufmann H. A TerraSAR-X InSAR study of landslides in southern Kyrgyzstan, Central Asia. *Remote Sensing Letters* 2013; 4: 657-666.
14. Shamshiri R, Motagh M, Baes M, Sharifi MA. Deformation analysis of the Lake Urmia causeway (LUC) embankments in northwest Iran: insights from multi-sensor interferometry synthetic aperture radar (InSAR) data and finite element modeling (FEM). *Journal of Geodesy* 2014; 88: 1171-1185.
15. Kampes BM, Hanssen RF, Perski Z. Radar interferometry with public domain tools In: *Proceedings of the Proceedings of FRINGE.* Year: 1-5.
16. Werner C, Wegmüller U, Strozzi T, Wiesmann A. Gamma SAR and interferometric processing software In: *Proceedings of the Proceedings of the ERS-Envisat symposium, gothenburg, Sweden.* Citeseer, Year: 1620.
17. Hooper A, Zebker HA. Phase unwrapping in three dimensions with application to InSAR time series. *JOSA A* 2007; 24: 2737-2747.
18. Hooper A, Zebker H, Segall P, Kampes B. A new method for measuring deformation on volcanoes and other natural terrains using InSAR persistent scatterers. *Geophysical research letters* 2004; 31.
19. Mateus P, Nico G, Tomé R, Catalao J, Miranda PM. Experimental study on the atmospheric delay based on GPS, SAR interferometry, and numerical weather model data. *IEEE Transactions on Geoscience and Remote Sensing* 2013; 51: 6-11.
20. Li Z, Ding X-L, Liu G. Modeling atmospheric effects on InSAR with meteorological and continuous GPS observations: algorithms and some test results. *Journal of Atmospheric and Solar-Terrestrial Physics* 2004; 66: 907-917.
21. Li Z, Fielding EJ, Cross P, Muller JP. Interferometric synthetic aperture radar atmospheric correction: GPS topography-dependent turbulence model. *Journal of Geophysical Research: Solid Earth* 2006; 111.
22. Vajedian S, Motagh M, Nilfouroushan F. StaMPS improvement for deformation analysis in mountainous regions: Implications for the Damavand volcano and Mosha fault in Alborz. *Remote Sensing* 2015; 7: 8323-8347.
23. Crosetto M, Monserrat O, Cuevas-González M, Devanthéry N, Luzi G, Crippa B. Measuring thermal expansion using X-band persistent scatterer interferometry. *ISPRS Journal of Photogrammetry and Remote Sensing* 2015; 100: 84-91.
24. Monserrat O, Crosetto M, Cuevas M, Crippa B. The thermal expansion component of persistent scatterer interferometry observations. *Geoscience and Remote Sensing Letters, IEEE* 2011; 8: 864-868.